Published February 28, 2019

Original Research

Core Ideas

- The accuracy of the PI method in estimating soil K_s was tested by numerical simulations.
- Estimated K_s using two-ponding-depth and multiple-ponding-depth infiltration were compared.
- Transient and steady-state infiltration data for six soils were used to estimate K_s.
- The PI should yield more accurate K_s estimates in coarse- than fine-textured soils.
- The transient method does not solve the K_s inaccuracy problems in fine-textured soils.

Accuracy of Saturated Soil Hydraulic Conductivity Estimated from Numerically Simulated Single-Ring Infiltrations

Vincenzo Bagarello, Massimo Iovino, and Jianbin Lai*

The single-ring pressure infiltrometer (PI) method is widely used to determine saturated soil hydraulic conductivity, K_s, directly in the field. The original and still most common way to analyze the data makes use of the steady-state model developed by the Canadian School in the 90s and two (two-ponding-depth, TPD, approach) or more (multiple-ponding-depth, MPD, approach) depths of ponding. The so-called Wu method based on a generalized infiltration equation allows analysis of the transient infiltration data collected by establishing a single ponding depth of water on the infiltration surface. This investigation, making use of simulated infiltration runs for initially unsaturated sand to silty clay loam soils, showed that, with a run duration of practical interest (e.g., 2 h), the PI can be expected to yield more accurate estimates of K_s in coarse-textured soils than in fine-textured soils even if the transient method is used instead of the steady-state method. Performing a three-level experiment and analyzing the estimated steady-state infiltration rates with both the TPD and MPD approaches is a way to predict the reliability of the estimated K_s value. The K_s accuracy should be acceptable if the two approaches yield similar results. Otherwise, the MPD approach should be expected to yield more accurate K_s estimates than the TPD approach. The transient method does not solve the K_s inaccuracy problems in fine-textured soils because obtaining accurate K_s data requires that the portion of total infiltration varying linearly with time represent a high percentage of total infiltration, but this percentage is small in fine-textured soils when the run does not exceed a few hours. This investigation opens some new perspective on the use of infiltration data to make predictions on the expected reliability of the K_s calculations with reference to both steady-state and transient data analysis procedures.

Abbreviations: L, loam; LS, loamy sand; MPD, multiple-ponding-depth; PI, pressure infiltrometer; S, sand; SAL, sandy loam; SCL, silty clay loam; SIL, silt loam; TPD, two-ponding-depth.

Saturated soil hydraulic conductivity, K_s, should be determined in situ for interpreting and simulating soil hydrologic processes since, in this case, the disturbance of the sampled soil volume is minimized and its functional connection with the surrounding soil is maintained (Bouma, 1982). Due to the high spatial variability of this soil property, a large number of individual determinations of K_s should be performed to characterize an area of interest at a given time (Reynolds and Zebchuk, 1996; Mallants et al., 1997; Bagarello et al., 2013a). The duration of a single run cannot be excessively long because the required field work should be practically sustainable.

In the last 30 yr, field soil hydraulic conductivity characterization by permeameters and infiltrometers has become very common, mainly thanks to the theoretical and practical developments by the Canadian school (Reynolds and Elrick, 1985, 1987, 1990, 1991; Reynolds et al., 1985, 1992). In particular, the single-ring pressure infiltrometer (PI) (Reynolds and Elrick, 1990) has been used in many investigations (Vauclin et al., 1994; Ciollaro and Lamaddalena, 1998; Bagarello and Iovino, 1999; Angulo-Jaramillo et al., 2000; Bagarello et al., 2000, 2013b, 2014; Reynolds et al., 2000; Mertens et al., 2002; Bagarello and Sgroi, 2004; Gómez et al., 2005; Verbist et al., 2009, 2010, 2013). The PI method uses a ring with a small radius that is inserted into the soil to a short depth. A constant depth of ponding, H, is established within the infiltration ring, and the flow rate

V. Bagarello and M. Iovino, Dip. di Scienze Agrarie Alimentari e Forestali, Univ. degli Studi di Palermo, Viale delle Scienze, Palermo 90128, Italy; J. Lai, Yucheng Comprehensive Experimental Station, Institute of Geographic Sciences and Natural Resources Research, Chinese Academy of Sciences, Beijing 100101, China, and State Key Lab. of Hydraulic and Mountain River Engineering (SKHL), Sichuan Univ., Chengdu 610065, China. *Corresponding author (laijianbin@igsnrr.ac.cn).

Received 21 June 2018.
Accepted 1 Nov. 2018.

Citation: Bagarello, V., M. Iovino, and J. Lai. 2019. Accuracy of saturated soil hydraulic conductivity estimated from numerically simulated single-ring infiltrations. Vadose Zone J. 18:180122. doi:10.2136/vzj2018.06.0122

into the soil is monitored. Three-dimensional, steady, ponded flow out of the ring is used to determine K_s by a model that takes hydrostatic pressure, capillarity, and gravity components of flow out of the ring into account (Reynolds and Elrick, 1990). The two- (TPD) and multiple-ponding-depth (MPD) approaches can be applied to determine K_s and the so-called matric flux potential, ϕ_m, using exclusively steady-state infiltration rates. The two approaches differ by the number of ponded depths of water that are established in succession on the infiltration surface, i.e., two or more than two.

Flow from infiltrometers into unsaturated soil goes through an initial transient phase of decreasing rates and then approaches steady state (Elrick and Reynolds, 1992b). Therefore, applying the steady-state model of Reynolds and Elrick (1990) needs the collection of reliable steady-state infiltration rate data. The equilibration time, or the time to near-steady-state conditions, depends on many factors. In particular, it generally increases with finer soil texture, drier initial soil conditions, and increasing depth of water ponding on the infiltration surface, along with the depth of cylinder insertion and ring radius (Reynolds et al., 2002a, 2002b; Reynolds, 2008). According to Reynolds and Elrick (2002), a reasonable estimate of steady flow, or quasi-steady flow, can generally be considered acceptable in natural environments and only early-time transient flow procedures are practicable if equilibration times are particularly long, i.e., many hours or even days.

It is not easy to assess if the estimated steady-state infiltration rates are reliable during a field application of the PI method. As a matter of fact, the criteria that can be applied to detect steady-state conditions are unavoidably approximate, and different criteria could yield a contrasting conclusion on the time to steady state (Bagarello et al., 1999; Bagarello and Giordano, 1999). In other words, in practical use of the method, a run of fixed duration does not assure attainment of a steady-state flow rate under any circumstance, but examining the data could be not enough to recognize that steady state was not reached. Therefore, it is necessary to establish what happens when the steady-state model of Reynolds and Elrick (1990) is used to analyze an infiltration run for which steady-state conditions are unavoidably estimated on the basis of the collected data. Working under initially more or less dry soil conditions has a particular interest since equilibration times are expected to be particularly long in this case but the run duration cannot exceed limits that are dictated by practical and environmental constraints. Indeed, only a few investigations making use of very long field runs can be found in the literature (e.g., Papanicolaou et al., 2015; Alagna et al., 2016).

A way to overcome equilibration time issues could be applying the so-called Method 1 by Wu et al. (1999) (referred to as the Wu method in the following) that uses the whole infiltration curve without discriminating between early-time and steady-state infiltration. This method has received little testing after its development (Reynolds and Elrick, 2002) and some of the tests that were made need to be complemented by other checks. In particular, Wu et al. (1999) successfully verified their method against simulated infiltration data. However, the run duration was 1 h for a sandy soil but 1 d for a sandy clay loam soil and 10 d for a clay soil. Testing the method against shorter runs is of more practical interest. Moreover, contrasting information can be found in the few studies dealing with the performance of this method. For example, Bagarello et al. (2009) and Verbist et al. (2010) concluded that the Wu method was a valid alternative to steady-state methods of analysis, but Di Prima et al. (2018) recognized that steady-state approaches performed better than the Wu method, mainly as a consequence of the difficulty in fitting the infiltration model to the data.

Numerical simulation of an infiltration process into an initially unsaturated porous medium is a powerful tool to test hypotheses and to check factors affecting the applicability of a particular analytical procedure to estimate soil characteristics (Bagarello et al., 2013b). For example, numerically simulated data were used by Wu et al. (1993) to explain erratic K_s estimates obtained by the borehole permeameter technique in soils with macropores and abrupt layers. Lai and Ren (2007) and Lai et al. (2010) used numerical simulation to improve the determination of K_s by the double-ring infiltrometer. Dušek et al. (2009) and Dohnal et al. (2016) analyzed numerically generated single-ring data to test the dependence of the infiltration rate on several factors, such as ring diameter, ring insertion depth, and ponding depth of water on the infiltration surface. Bagarello et al. (2013b) used numerical simulation to test the performance of the TPD approach for PI data collected in heterogeneous soils. Numerically simulated data were used by Reynolds (2013) to assess different borehole infiltration analyses for determining K_s in the vadose zone. Bagarello et al. (2016) used numerical simulation of a single-ring infiltration process to test the single-level, steady-state analysis developed for the PI (Reynolds and Elrick, 1990).

In practical application of the PI method, the run duration is generally fixed in advance, and it is in most cases short or relatively short since it does not exceed a few hours at the most. The available water volume for the run is also fixed in advance, especially for applications in remote areas, and even in this case the run duration has to be expected to be rather short. Possibly, the collected data will allow an estimate of the steady-state flow rate, but they will also appear to be analyzable with a method that does not distinguish between early-time and steady-state infiltration. Establishing what is the best way to determine K_s in such situations could improve routine use of the PI method in the field.

The general objective of this investigation was to check procedures for determining K_s with numerically simulated single-ring PI runs for a variety of soils. The specific objectives were (i) to test the performances of both steady-state and transient methods of analysis, and (ii) to verify if the collected infiltration data can be used to make a prediction about the reliability of the estimated K_s.

Theory

The approximate analytical expression for steady, ponded flow out of a ring into rigid, homogeneous, isotropic, uniformly unsaturated soil is (Reynolds and Elrick, 1990)

$$Q_s = \frac{r}{G}\left(K_s H + \phi_m\right) + \pi r^2 K_s \quad [1]$$

where Q_s [L^3 T^{-1}] is the steady-state flow rate, r [L] is the ring radius, K_s [L T^{-1}] is the saturated soil hydraulic conductivity, H [L] is the steady depth of water ponding in the ring, and ϕ_m [L^2 T^{-1}] is the matric flux potential, defined as (Gardner, 1958)

$$\phi_m = \int_{h_i}^{0} K(h)\,dh \qquad -\infty \le h_i \le 0 \quad [2]$$

where $K(h)$ [L T^{-1}] is the soil hydraulic conductivity vs. pressure head, h [L], relationship and h_i [L] is the initial pressure head. The dimensionless shape factor, G, takes into account the complex interactions between ring radius, depth of ring insertion, d [L], depth of ponding in the ring, soil capillarity, and gravity. The values of the shape factor were determined numerically for selected porous media (sand, loam, and clay soils and clay cap or liner) and H–d–r combinations (Reynolds and Elrick, 1990). The G values were found to be nearly independent of soil hydraulic properties and H for $H \ge 0.05$ m. Therefore, the following relationship was developed to estimate G (G_e):

$$G_e = 0.316\frac{d}{r} + 0.184 \quad [3]$$

Two different approaches can be used to simultaneously determine K_s and ϕ_m of Eq. [1], depending on the number of the applied steady depths of water ponding during the experiment (Reynolds and Elrick, 1990).

The TPD approach requires the steady-state flow rates, Q_{s1} and Q_{s2}, corresponding to two ponding depths of water, H_1 and H_2 ($H_2 > H_1$), consecutively established on the infiltrating surface, i.e., without occurrence of a drainage phase in the passage from H_1 to H_2. If only the effect of the ring radius and the insertion depth on the shape factor is accounted for by Eq. [3], the following relationships can be applied to calculate K_s, ϕ_m, and the so-called α^* [L^{-1}] parameter:

$$K_s = \frac{G_e}{r}\left(\frac{Q_{s2} - Q_{s1}}{H_2 - H_1}\right) \quad [4]$$

$$\phi_m = \frac{G_e}{r}\left(\frac{H_2 Q_{s1} - H_1 Q_{s2}}{H_2 - H_1} - \pi r G_e \frac{Q_{s2} - Q_{s1}}{H_2 - H_1}\right) \quad [5]$$

$$\alpha^* = \frac{K_s}{\phi_m} \quad [6]$$

The MPD approach uses two or more H levels and Eq. [1] written in the form

$$Q_s = \left(\pi r^2 K_s + \frac{r\phi_m}{G_e}\right) + \frac{rK_s}{G_e} H \quad [7]$$

Therefore, the slope, b_1, and the intercept, b_0, of the linear least-squares regression line through a plot of Q_s vs. H allow the two unknowns to be obtained:

$$K_s = \frac{b_1 G_e}{r} \quad [8]$$

$$\phi_m = \frac{G_e}{r}\left(b_0 - \pi r^2 K_s\right) \quad [9]$$

Equation [6] can then be used to estimate α^*. The MPD experiment is expected to have an advantage over the TPD experiment. In particular, with the former approach, random variability in Q_s due to measurement error or small-scale heterogeneity tends to be filtered out by the regression line (Reynolds and Elrick, 1990). This filtering is probably not very important when the PI run is numerically simulated, but it may have interest if the data are collected under real field conditions.

The Wu method (Wu et al., 1999) is based on the assumption that the following cumulative infiltration curve can be used to describe the infiltration process:

$$I = A_w t + B_w t^{0.5} \quad [10]$$

where I [L] is cumulative infiltration, t [T] is time and A_w [L T^{-1}] and B_w [L T$^{-0.5}$] are the curve parameters. Equation [10] is fitted to the (t, I) data pairs measured from the beginning of the PI experiment to obtain an estimate of A_w and B_w. Then, K_s is given by

$$K_s = \frac{\Delta\theta\left[\sqrt{(H + G^*)^2 + 4G^* C} - (H + G^*)\right]}{2T_c} \quad [11]$$

where $\Delta\theta$ [L^3 L^{-3}] is the difference between the saturated volumetric soil water content, θ_s [L^3 L^{-3}], and the initial volumetric soil water content, θ_i [L^3 L^{-3}] and the G^* [L], C [L], and T_c [T] terms have the following expressions:

$$G^* = d + \frac{r}{2} \quad [12a]$$

$$C = \frac{1}{4\Delta\theta}\left(\frac{B_w}{b}\right)^2 \frac{a}{A_w} \quad [12b]$$

$$T_c = \frac{1}{4}\left(\frac{B_w a}{b A_w}\right)^2 \quad [12c]$$

where a and b are dimensionless constants ($a = 0.9084$, $b = 0.1682$). An estimate of the α^* parameter may be obtained by the following relationship:

$$\alpha^* = \frac{K_s}{\phi_m} \approx \frac{K_s}{\phi'_m} \quad [13]$$

where ϕ'_m (L^2 T^{-1}) is the matric flux potential calculated with a modified van Genuchten hydraulic conductivity–pressure head function. The Gardner (1958) hydraulic conductivity function was considered by Reynolds and Elrick (1990) but, according to Eq. [13], the choice of the hydraulic conductivity function doesn't have a significant impact on the calculation of α^*. The ϕ'_m term is given by

$$\phi'_m = \frac{K_s^2 T_c}{\Delta\theta} \quad [14]$$

Materials and Methods

Soils and Numerical Simulations

Numerical simulations were performed for the six homogeneous soils considered by Hinnell et al. (2009). Soil hydraulic properties were modeled according to the van Genuchten–Mualem model (Mualem, 1976; van Genuchten, 1980), with hydraulic parameters taken from Carsel and Parrish (1988) (Table 1):

$$\Theta(h)=\frac{\theta(h)-\theta_r}{\theta_s-\theta_r}=\left(1+\left|\alpha_{vG}h\right|^n\right)^{-m} \qquad m=1-\frac{1}{n} \qquad [15a]$$

$$K(h)=K_s\Theta^{0.5}\left[1-\left(1-\Theta^{1/m}\right)^m\right]^2 \qquad [15b]$$

where Θ is the effective saturation, h [L] is the soil water pressure head, θ [$L^3\ L^{-3}$] is the volumetric soil water content, θ_s [$L^3\ L^{-3}$] and θ_r [$L^3\ L^{-3}$] are the saturated and residual volumetric soil water contents, respectively, α_{vG} [L^{-1}], m, and n are soil-specific empirical parameters of the van Genuchten–Mualem model, K [$L\ T^{-1}$] is the unsaturated soil hydraulic conductivity, and K_s [$L\ T^{-1}$] is the saturated soil hydraulic conductivity. These soils were considered to be appropriate for studying a three-dimensional infiltration process into an initially unsaturated porous medium from a small-size source (Hinnell et al., 2009). Moreover, the selected soils differed widely by their hydraulic properties, allowing exploration of a wide range of situations, including those where equilibration times of the ponding infiltration run are expected to be rather long (Reynolds, 2008).

A two-dimensional axisymmetric vertical flow domain was adopted for all the simulations using the HYDRUS-2D/3D software package (Šimůnek et al., 2007), which is widely used for simulating water, heat, and/or solute movement in two or three dimensions (Shan and Wang, 2012; Chen et al., 2015; Bautista et al., 2016; Rezaei et al., 2016). The dimensions of the flow domain were 50 cm in the x direction and 100 cm in the z direction for all soils except the silt loam (SIL) and silty clay loam (SCL) soils. A smaller size of flow domain, i.e., 30 by 50 cm, was adopted for the SIL and SCL soils to ensure the simulations could run properly with the finest possible mesh size to improve computation efficiency and reduce the mass balance errors. Moreover, a variable mesh size of finite elements was used that was generated using the MESHGEN subroutine embedded in the HYDRUS-2D/3D software package. A mesh size of 0.05 cm was adopted for the zone from 0 cm (surface) to the 3-cm depth of the flow domain. The mesh size was then gradually increased to a maximum of 2.64 cm (or 0.41 cm for the SCL soil) for the deeper part of the flow domain.

For a given soil and an established initial soil water content, different PI runs were simulated by considering a ring having a radius r = 75 mm. For this reason, a notch was generated 75 mm away from the origin in the x direction on top of the flow domain to represent the infiltrometer wall. The notch was 5 mm in width and 30 mm in depth, which is equal to the insertion depth of the ring. A ring insertion depth d = 0 mm was also considered for some simulations. Both the outer border and the bottom of the flow domain were far away from the possible wetting zone. Therefore, both the lateral and bottom boundaries had negligible effect on the infiltration process. A constant head of water was established for the upper boundary condition of the infiltration zone, whereas the bottom condition of the flow domain was free drainage. The boundary condition on the infiltrometer wall (notch) and on the unconfined soil surface was no flux. A uniform distribution of the soil water content in the form of a water head was selected for the initial conditions of all the simulations.

A variable time step was adopted to reduce the computation time while assuring simulation accuracy. The initial, minimum, and maximum time steps were 0.01, 0.01, and 60 s, respectively. The absolute water content tolerance was 0.0005 (0.05%), the absolute pressure head tolerance was 0.5 cm, and the maximum number of iterations allowed during any time step was 10. With the chosen spatiotemporal discretization, the mass balance error was <0.203% for most cases, but it did not exceed 1.08% for all simulations used in this investigation. Haverkamp et al. (1977) compared different numerical schemes and considered as "good" or "excellent" mass balance errors in the range from 0.2 to 0.4%. Reynolds (2010, 2011) obtained mass balance errors of $\leq$ 0.05% and concluded that this level of error was acceptable because it was well below the commonly accepted upper limit of 0.1 to 1% for soil and groundwater flow. Therefore, our simulations were considered acceptable according to the existing evaluation criteria (Celia et al., 1990; Rathfelder and Abriola, 1994; Jacques et al., 2006)

Three different sets of infiltration data were numerically simulated in this investigation. In particular, the 3Hd30 dataset was developed by considering a ring insertion depth d = 30 mm and three constant heads of water—H_1 = 50 mm, H_2 = 100 mm, and H_3 = 200 mm—that were established in succession, without any allowed drainage in the passage from one H value to the next. For the H100d30 dataset, d was equal to 30 mm and the single depth of ponding was H = 100 mm. For the H50d0 dataset, d = 0

Table 1. Parameters† of the van Genuchten–Mualem soil hydraulic model (Carsel and Parrish, 1988; Hinnell et al., 2009) and α^* parameter for two values of the initial effective saturation Θ_i.

Soil	θ_r	θ_s	α_{vG}	n	m	K_s	α^* $\Theta_i = 0.05$	α^* $\Theta_i = 0.4$
	– $m^3\ m^{-3}$ –		cm^{-1}			$mm\ h^{-1}$	—— mm^{-1} ——	
Sand	0.045	0.43	0.145	2.68	0.627	297.0	0.0263	0.0265
Loamy sand	0.057	0.41	0.124	2.28	0.561	145.9	0.0260	0.0263
Sandy loam	0.065	0.41	0.075	1.89	0.471	44.2	0.0201	0.0203
Loam	0.078	0.43	0.036	1.56	0.359	10.4	0.0144	0.0145
Silt loam	0.067	0.45	0.020	1.41	0.291	4.5	0.0112	0.0112
Silty clay loam	0.089	0.43	0.010	1.23	0.187	0.7	0.0117	0.0117

† θ_r, residual volumetric soil water content; θ_s, saturated volumetric soil water content; α_{vG}, n, and m, soil-specific empirical parameters of the van Genuchten–Mualem model; K_s, saturated soil hydraulic conductivity; α^* parameter; $\Theta_i = (\theta_i - \theta_r)/(\theta_s - \theta_r)$, where θ_i ($m^3 m^{-3}$) is the initial or antecedent volumetric soil water content.

and $H = 50$ mm were considered. A given H value was maintained for 120 min because this run duration was considered to be an acceptable compromise between the need to obtain reliable estimates of the steady-state flow rate and the fact that excessively long runs could be of reduced interest, being impractical in the field (Reynolds et al., 2000; Mertens et al., 2002; Verbist et al., 2013). Two different values of the initial effective saturation ($\Theta_i = 0.05$ and 0.4, i.e., dry and intermediate conditions, respectively) were considered for each simulated run.

Calculations and Data Analysis

A soil was characterized by a theoretical value of the saturated hydraulic conductivity and two theoretical values (one for each Θ_i condition) of both the matric flux potential and the α^* parameter. For a given Θ_i, the theoretical ϕ_m value was calculated by numerical integration of Eq. [2]. The water content range from initial water content to saturation was subdivided into 10^5 equally spaced intervals and pressure head values, h_{i-1} and h_i ($i = 1, 2, ..., 10^5$), corresponding to the extremes of each interval calculated by Eq. [15a]. The trapezium rule was then used to calculate the area under the hydraulic conductivity curve by means of an automated Microsoft Excel routine.

Cumulative infiltration volumes [L^3] and flow rates [$L^3 T^{-1}$] obtained by numerical simulations were transformed into infiltrated depths of water, I (mm), and infiltration rates, i_r (mm h^{-1}), respectively, by dividing volumes by the infiltration surface, since reasoning in terms of I and i_r is more practical to manage infiltration data. Consequently, the steady-state flow rate obtained by Eq. [1] was also transformed into a steady-state infiltration rate by the $i_s = Q_s/(\pi r^2)$ relationship. The numerically simulated cumulative infiltration curves were used to obtain an estimate of i_s by considering the last 20 min of the process with a given H and determining the slope of the linear regression line fitted to the (I, t) data pairs (Bagarello et al., 1999).

Simultaneous calculation of K_s (mm h^{-1}) and ϕ_m (mm^2 h^{-1}) was performed using both the TPD approach with $H_1 = 50$ mm and $H_2 = 100$ mm and the MPD approach with $H_1 = 50$ mm, $H_2 = 100$ mm, and $H_3 = 200$ mm to check the performance of the two tested approaches, although they are expected to yield similar results under ideal conditions (Reynolds and Elrick, 1990). The estimated K_s values were compared with the corresponding theoretical values. According to the accuracy criterion of Reynolds (2013), the estimates were deemed accurate when they fell within the range $0.75 \leq K_r = K_{s,estimated}/K_{s,true} \leq 1.25$ (i.e., <25% error).

The Wu method was tested by considering cumulative infiltration for $H = 50$ mm and $d = 30$ mm (the H50d30 scenario; dataset extracted from the previously developed 3Hd30 dataset), $H = 100$ mm and $d = 30$ mm (H100d30), and $H = 50$ mm and $d = 0$ (H50d0). The r, d, and H values for the first two scenarios were consistent with those considered by Wu and Pan (1997) for checking their infiltration model ($60 \leq r \leq 200$ mm, $20 \leq d \leq 100$ mm, and $0 \leq H \leq 200$ mm). The null insertion depth of the ring considered for the third scenario was close to the lowest considered value of d (Wu and Pan, 1997) and was included in this check due to the implications for the infiltration process (Dohnal et al., 2016). More clearly, infiltration is initially confined and then unconfined with $d > 0$, but it is always unconfined with $d = 0$. Estimation of A_w and B_w was performed by the least squares optimization technique of nonlinear fitting of Eq. [10] on the (I, t) data set (Wu et al., 1999; Lassabatére et al., 2006), although this technique does not allow undoubted establishment of whether Eq. [10] fits the I vs. t data adequately (Vandervaere et al., 2000). Linearization of the infiltration model was proposed as a way to check the adequacy of Eq. [10] (Smiles and Knight, 1976; Vandervaere et al., 2000), and, in a field test of the Wu method on a sandy loam soil, linearization yielded similar results to those obtained by nonlinear fitting (Bagarello et al., 2009). However, linearization was checked in this investigation only for the H50d0 scenario because, using numerically simulated infiltration data, Dohnal et al. (2016) showed that, with an insertion depth >0, a single straight line does not describe the entire infiltration process. The quality of the fit was evaluated by calculating the relative error, Er:

$$\mathrm{Er} = \sqrt{\frac{\sum_{i=1}^{k}\left(I_e - I_m\right)^2}{\sum_{i=1}^{k} I_m^2}} \qquad [16]$$

where k is the number of considered data points, I_e is the estimated cumulative infiltration, and I_m is the numerically simulated cumulative infiltration. According to Lassabatére et al. (2006), Er $\leq$ 3.5% denotes a satisfactory fitting of the model to the data. Equation [10] was fitted to the (I, t) data by considering different durations for each run to also see if the field test could conveniently be shortened when a transient method of analysis is applied. In particular, the considered durations were 120, 90, 60, and 30 min. Therefore a total of 144 (A_w, B_w) data pairs were obtained (3 scenarios $\times$ 6 soils $\times$ 2 initial soil water conditions $\times$ 4 run durations). Equations [11–14] and [6] were used to calculate K_s and α^* for each considered infiltration process.

Results and Discussion

Theoretical Values of the α^* Parameter

The considered discretization of the $K(h)$ function allowed an accurate estimation of ϕ_m, given that the pressure head interval was always <36.3 mm. The theoretical α^* values determined by Eq. [6] varied from 0.0112 to 0.0265 mm^{-1} for soils with $0.7 \leq K_s \leq 297$ mm h^{-1} (Table 1). According to Reynolds and Elrick (1990) and Elrick and Reynolds (1992a), $\alpha^* = 0.012$ to 0.036 mm^{-1} is expected for coarse- and medium-textured soils having K_s values that range between 3.6 and 360 mm h^{-1}. A lower α^* value, i.e., 0.004 mm^{-1}, should be typical of fine-textured soils with $K_s = 0.036$ mm h^{-1}, which is approximately 20 times lower than the lowest K_s value considered in this investigation. Therefore, this check of the theoretical α^* calculations did not reveal unexpected values.

Steady-State Method

Both the TPD and the MPD approach yielded simultaneously positive K_s and α^* values for each soil–Θ_i combination (Table 2). In particular, α^* varied from 0.00036 to 0.048 mm^{-1} with the TPD approach (<0.001 mm^{-1} only with reference to the SCL soil and $\Theta_i = 0.05$) and from 0.0036 to 0.036 mm^{-1} with the MPD approach. Simultaneously positive K_s and α^* values denote a successful experiment (Reynolds and Elrick, 1990), but only the runs yielding both positive results for both variables and α^* values ranging from 0.001 to 0.1 m^{-1} should be considered reliable according to a later suggestion by Reynolds and Elrick (2002). With this more stringent criterion, the only possible uncertainty in the reliability of the K_s and α^* calculations was detected with reference to a two-level experiment performed on the finest soil under the driest initial conditions.

Excluding the SCL soil, accurate estimates of K_s ($0.75 \leq K_r \leq 1.25$) were always obtained regardless of the considered data analysis procedure and the initial soil water content. This result was consistent with the conclusion of Reynolds and Elrick (1990) that a similar K_s accuracy level has to be expected with the TPD and MPD approaches, and it was a consequence of the similarity between the i_s values estimated at the end of the simulated run, i_{sES}, and the predicted i_s values by Eq. [1] and [3], i_{sRE}, i.e., according to the steady-state model of Reynolds and Elrick (1990) (i.e., differences never exceeding 5%). In other terms, each i_{sES} value was close to the expected steady-state infiltration rate because steady-state conditions were achieved at the end of the infiltration run. The reason why $\Delta i_s = 100(i_{sES} - i_{sRE})/i_{sRE} \leq 5\%$ was considered small calls for an explanation. With reference to the porous medium–d–r–H combinations of Reynolds and Elrick (1990, their Table 2), using Eq. [1] and two alternative G factors, i.e., the numerically calculated G value reported in that table and the corresponding estimate by Eq. [3] yielded i_s values differing by up to 17%. Therefore, $\Delta i_s \leq 5\%$ was small because this value was appreciably lower than a negligible 17% according to the analysis developed by Reynolds and Elrick (1990).

Table 2. Saturated hydraulic conductivity, K_s, and α^* parameter obtained with the two-ponding-depth (TPD) and multiple-ponding-depth (MPD) approaches for different soils and initial effective saturation (Θ_i) values.

Soil	Θ_i	TPD approach		MPD approach	
		K_s	α^*	K_s	α^*
		mm h^{-1}	mm^{-1}	mm h^{-1}	mm^{-1}
Sand	0.05	333.8	0.0416	318.8	0.0313
	0.4	333.7	0.0415	319.2	0.0316
Loamy sand	0.05	164.2	0.0464	158.0	0.0357
	0.4	164.7	0.0477	158.2	0.0361
Sandy loam	0.05	48.6	0.0331	47.5	0.0292
	0.4	49.4	0.0385	47.7	0.0317
Loam	0.05	10.8	0.0166	10.9	0.0171
	0.4	10.9	0.0190	10.9	0.0188
Silt loam	0.05	4.31	0.0090	4.78	0.0117
	0.4	4.62	0.0120	4.69	0.0125
Silty clay loam	0.05	0.081	0.00036	0.558	0.00357
	0.4	0.391	0.00266	0.658	0.00606

For the SCL soil, the estimates of K_s were accurate with the MPD approach ($K_r = 0.80$ and 0.94 for $\Theta_i = 0.05$ and 0.4, respectively) but not with the TPD approach ($K_r = 0.12$ and 0.56). To establish the reason why the two approaches had a different performance, it was initially recognized that, for this soil, large Δi_s values were generally obtained. In particular, Δi_s decreased from 60.5 to 24.8% in the passage from H_1 to H_3 for $\Theta_i = 0.05$ and from 33.4 to 15.9% for $\Theta_i = 0.4$. Therefore, i_s was overestimated in general, denoting that the runs were too short to allow attainment of near-steady-state conditions.

Time to steady state is known to increase with the depth of water ponding (Reynolds, 2008), which could not appear consistent with an i_s overestimation decreasing with larger H values. However, it should be considered that, for $H_1 = 50$ mm, i_s was estimated by a 120-min infiltration run but the i_s estimate corresponding to a larger value of H (e.g., $H_3 = 200$ mm) was obtained with a longer run (120 × 3 = 360 min). In other terms, overestimation of i_s decreased with H because the run duration increased. To test this explanation, the i_s overestimation detected for $H = 100$ mm with the three-level experiment (32% for $\Theta_i = 0.05$ and 18% for $\Theta_i = 0.4$) was compared with that associated with a 4-h run steadily performed with $H = 100$ mm (28 and 16% for $\Theta_i = 0.05$ and 0.4, respectively). Corresponding Δi_s values were similar but they were slightly higher in the former case. This result was consistent with the fact that 2 of the 4 h were performed with a smaller H level in the former case. Another check was made by comparing, for $H = 100$ mm, the i_s overestimation associated with the three-level experiment with that obtained with an infiltration process of 2 h established on a SCL soil maintained at $\Theta_i = 0.05$ and $\Theta_i = 0.4$. An appreciably higher overestimation of i_s (57% for $\Theta_i = 0.05$ and 34% for $\Theta_i = 0.4$) was detected in this last case, further confirming that the initial run with a smaller water level implied less i_s overestimation for the larger H level. Therefore, the suggested explanation for an overestimation of i_s decreasing in the passage from the lowest to the highest H values was supported by the checks that were performed.

A noticeable improvement of the calculated K_s values was detected when the MPD approach was applied instead of the TPD one, especially for $\Theta_i = 0.05$, indicating that even large overestimations of i_s for all established ponded depths of water did not prevent accurate calculations of K_s. Moreover, two overestimated i_s values yielded inaccurate results (TPD approach) but exactly these two estimates plus an additional, still overestimated, i_s value (MPD approach) adjusted the K_s calculation.

Little faith should be placed in a good result obtained by a fortuitous cancellation of errors (Smettem et al., 1995), which means that the PI method should not be applied, regardless of the experimental and data analysis procedures (TPD or MPD), if there is a sound suspect that steady state was not reached at the end of the run (Reynolds and Elrick, 2002). However, explaining why the applied approach had a noticeable impact on the reliability of the K_s estimates was expected to improve our knowledge about the potential and limitations of the PI method. Equations [4] (TPD approach) and [8] (MPD approach) have exactly the same mathematical form, only difference being that the $\Delta Q/\Delta H$ gradient is calculated with reference to two successively ponded depths of water in the former case and to all established ponded depths of water (three in this investigation) in the latter case. An error-free calculation of K_s, i.e., $K_r = 1$, needs using a $\Delta Q/\Delta H$ gradient of 169 mm^2 h^{-1} for the SCL soil. With the TPD approach, this gradient was underestimated by 88.5% for $\Theta_i = 0.05$ and 44.1% for $\Theta_i = 0.4$. With the MPD approach, underestimation decreased to 20.3 and 5.9%, respectively (Fig. 1). Therefore, the reliability of the estimates was better for the three-level experiment because the addition of a third i_s value reduced the discrepancy between the expected and the estimated $\Delta Q/\Delta H$ gradient for both values of the antecedent soil water content.

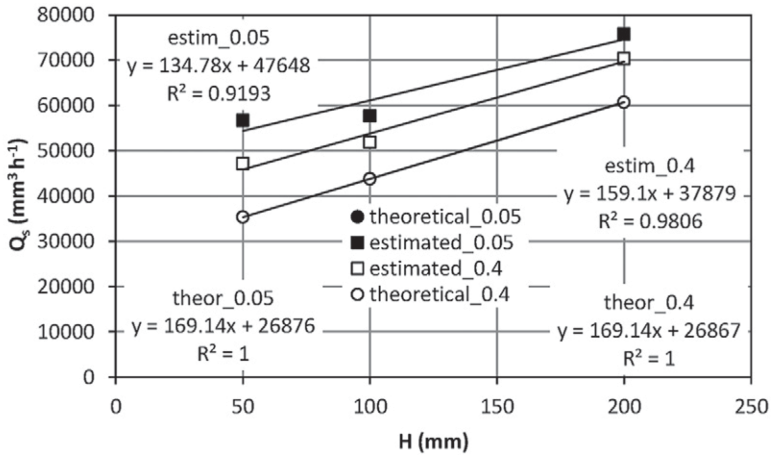

Fig. 1. Steady-state flow rate, Q_s, against ponded depth of water on the infiltration surface, H, for a three-level experiment in the silty clay loam soil with an initially dry (initial effective saturation $\Theta_i = 0.05$) and intermediate ($\Theta_i = 0.4$) soil water content (no distinguishable differences between the theoretical values of Q_s for any given H).

According to this investigation, performing a three-level experiment and analyzing the estimates of i_s with both the TPD and MPD approaches should be recommended for practical use of the PI method. If the two approaches yield similar estimates of K_s, we can be rather confident that near-steady-state conditions were reached for each established H level and that the estimate of K_s is accurate. Establishing more than two ponding depths of water was not necessary to accurately estimate K_s, but this information was not available before making the experiment. If an appreciably lower K_s value is obtained with the TPD approach compared with the MPD one, then we should think that the latter approach yielded a more accurate estimate of K_s than the former one but also that overestimation of i_s occurred for the established H levels. In other terms, the MPD approach yields the estimate of K_s. The comparison between this approach and the TPD one allows establishment of whether the K_s calculations are based on reliable estimates of steady-state flow rates.

Transient Method

The infiltration model, i.e., Eq. [10], described well the data because Er did not exceed 1.2% for the H50d30 scenario ($N = 48$ runs, 6 soils × 2 initial soil water conditions × 4 run durations), 1.6% for the H100d30 scenario, and 0.6% for the H50d0 scenario. However, a good fit did not necessarily imply that the K_s estimates were accurate.

In particular, the estimates of K_s were poor for the three finest textured soils, i.e., the loam (L), SIL, and SCL, for the two Θ_i values when the simulated durations were 0.5 to 2 h (Table 3). In these cases, $K_r < 0.75$ was generally obtained but, in some cases (SCL soil, H50d30 and H100d30 scenarios, run durations ≤1.5 h), estimating K_s was not possible because the estimated A_w parameter was equal to zero, which denoted the inability of Eq. [10] to describe the data.

On the other hand, the K_s estimates were generally accurate for the three coarsest textured soils, i.e., the sand (S), LS, and sandy loam (SAL), since $0.75 \leq K_r \leq 1.25$ was obtained for 56 of the 72 considered runs (3 soils × 3 scenarios × 2 Θ_i values × 4 durations), i.e., in 78% of the cases. The H100d30 scenario performed better than the other two scenarios because K_s was accurately estimated in 92% of the cases (22 out of 24) with the former scenario and in 71% of the cases in the latter ones. The run duration was uninfluential in terms of K_s accuracy in 9 of the 18 considered cases (3 soils × 3 scenarios × 2 Θ_i values), whereas reducing the duration of the run determined a worsening (improvement) of the K_s estimates in seven (two) cases. An effect of Θ_i was not detected with reference to the H100d30 scenario. For the other two scenarios, a long or relatively long run (1.5–2.0 h) yielded accurate results when the S soil was initially dry but not when it was wet. For the SAL soil, a shorter run (1.5 h) than the longest one was usable to obtain accurate data only under wet conditions.

Therefore, with a run duration not exceeding 2 h, the Wu method did not yield accurate K_s values in fine-textured soils (L, SIL, SCL) regardless of the applied experimental methodology and initial wetness conditions. Estimates of K_s were generally accurate in coarser textured soils (S, LS, SAL). Run success percentages did not change by varying the ring insertion depth (H50d30 and H50d0 scenarios), but, for a given ring insertion depth, more hydrostatic pressure for the run was beneficial for accurately estimating K_s in these soils (H50d30 and H100d30 scenarios) because it determined a reduced sensitivity to both initial wetness and run duration compared with the other tested scenarios.

Figure 2 shows the infiltration curves for the two 2-h runs yielding the most (LS soil, $\Theta_i = 0.05$) and the least (SCL soil, $\Theta_i = 0.05$) accurate estimates of K_s with the H50d0 scenario. In this case, the ring insertion depth was null and therefore an impediment to linearization of the cumulative infiltration curve (Dohnal et al., 2016) was not expected. Plotting the data on an I vs. t plot

Table 3. Ratio K_r between the saturated soil hydraulic conductivity, K_s, estimated by the transient method and the true K_s value for different soils , initial effective saturation (Θ_i) values, and run durations. The italicized ratios fall within the accuracy range, i.e., 0.75 to 1.25 (Reynolds, 2013).

		$\Theta_i = 0.05$				$\Theta_i = 0.4$			
Scenario†	Soil‡	2.0 h	1.5 h	1.0 h	0.5 h	2.0 h	1.5 h	1.0 h	0.5 h
H50d30	S	*1.18*	*1.13*	*1.05*	*0.91*	1.26	*1.22*	*1.15*	*1.02*
	LS	*1.02*	*0.97*	*0.88*	0.74	*1.12*	*1.07*	*0.99*	*0.84*
	SAL	*0.76*	0.71	0.62	0.46	*0.85*	*0.80*	0.72	0.57
	L	0.46	0.39	0.29	0.15	0.57	0.50	0.40	0.24
	SIL	0.26	0.20	0.12	0.04	0.38	0.30	0.21	0.09
	SCL	0.01	NA§	NA	NA	0.04	0.02	0.01	NA
H100d30	S	*1.19*	*1.15*	*1.10*	*0.98*	*1.24*	*1.22*	*1.17*	*1.07*
	LS	*1.08*	*1.03*	*0.97*	*0.85*	*1.15*	*1.11*	*1.05*	*0.94*
	SAL	*0.87*	*0.83*	*0.75*	0.60	*0.95*	*0.91*	*0.84*	0.71
	L	0.61	0.53	0.42	0.24	0.71	0.65	0.55	0.36
	SIL	0.38	0.29	0.19	0.06	0.51	0.43	0.31	0.14
	SCL	0.003	NA	NA	NA	0.05	0.01	NA	NA
H50d0	S	*1.21*	*1.16*	*1.07*	*0.92*	1.31	1.26	*1.18*	*1.03*
	LS	*1.03*	*0.97*	*0.89*	*0.76*	*1.14*	*1.08*	*0.99*	*0.85*
	SAL	*0.75*	0.71	0.67	0.60	*0.83*	*0.78*	0.72	0.65
	L	0.59	0.57	0.55	0.50	0.63	0.61	0.58	0.53
	SIL	0.56	0.54	0.51	0.45	0.59	0.57	0.55	0.50
	SCL	0.36	0.32	0.25	0.10	0.43	0.40	0.36	0.27

† H is the ponding depth (mm) and d is the ring insertion depth (mm).
‡ S, sand; LS, loamy sand; SAL, sandy loam; L, loam; SIL, silt loam; SCL, silty clay loam.
§ NA, estimation of K_s was not possible.

did not reveal any particular anomaly, and both runs appeared analyzable by fitting Eq. [10] to the data. However, the $I/t^{0.5}$ vs. $t^{0.5}$ relationship was practically linear for the LS run but not for the SCL run because a clear curvature in the early phase of the run was perceived in this latter case. According to Smiles and Knight (1976) and Vandervaere et al. (2000), this result indicates that Eq. [10] was adequate to describe the data in the LS soil but not in the SCL soil. An upward concavity of the I vs. $t^{0.5}$ relationship was evident for the LS run but not for the SCL run because the relationship was nearly linear in this case. This last result suggested that Eq. [10] was not appropriate to describe infiltration in the fine-textured soil because soil capillarity controlled the first 2 h of infiltration (Cook and Broeren, 1994; Angulo-Jaramillo et al., 2016).

This finding suggested a test of the hypothesis that a link could be established between the reliability of the K_s estimate and the relative importance of the two terms in Eq. [10], i.e., $A_w t$ and $B_w t^{0.5}$. For each scenario, Fig. 3 shows K_r vs. the relative weight of the $A_w t$ term on total infiltration, i.e., $(A_w t)/(A_w t + B_w t^{0.5})$, at the end of the infiltration run. A weight of $A_w t$ that does not reach approximately the 75 to 82% of total infiltration, depending on the scenario, does not allow accurate estimates of K_s to be obtained that are too low compared with the true values. A weight greater than 97 to 98% of the total infiltration implies an unacceptable overestimation of K_s, i.e., $K_r > 1.25$. Therefore, the estimates of K_s are accurate for a weight of the $A_w t$ term, varying between 75 to 82 and 97 to 98%, and the considered scenario has a minor impact on the accuracy range because K_r vs. the relative weight of the $A_w t$ term relationships obtained for the three considered scenarios showed clear similarities (Fig. 3). According to this investigation, it seems possible to make a prediction of the expected reliability of the K_s estimate during a run of pre-established duration.

Estimating the A_w and B_w parameters of the infiltration model during the run is not a particularly complicated task, even during a field run. The weight of the two terms of the model varies with the run duration (Fig. 4), which implies that, at least to a certain degree and in some situations, it could be possible to adjust the duration of the run in an attempt to obtain a weight of the $A_w t$ term of 82 to 97%, assuring, at least in the context of this investigation, accurate estimates of K_s.

This investigation could explain why the estimates of K_s obtained by Wu et al. (1999) were all in an acceptable range according to those researchers. Probably this conclusion was correct because their K_s values were obtained from much longer simulation durations for the finer soils. In any case, an infiltration run of one or more days is of limited interest for practical application of the device, which suggests that, according to this investigation, the Wu method appears usable with good expected results in coarse to relatively coarse soils but not in fine soils.

In this investigation, more accurate estimates of K_s were generally obtained with a steady-state approach than a transient

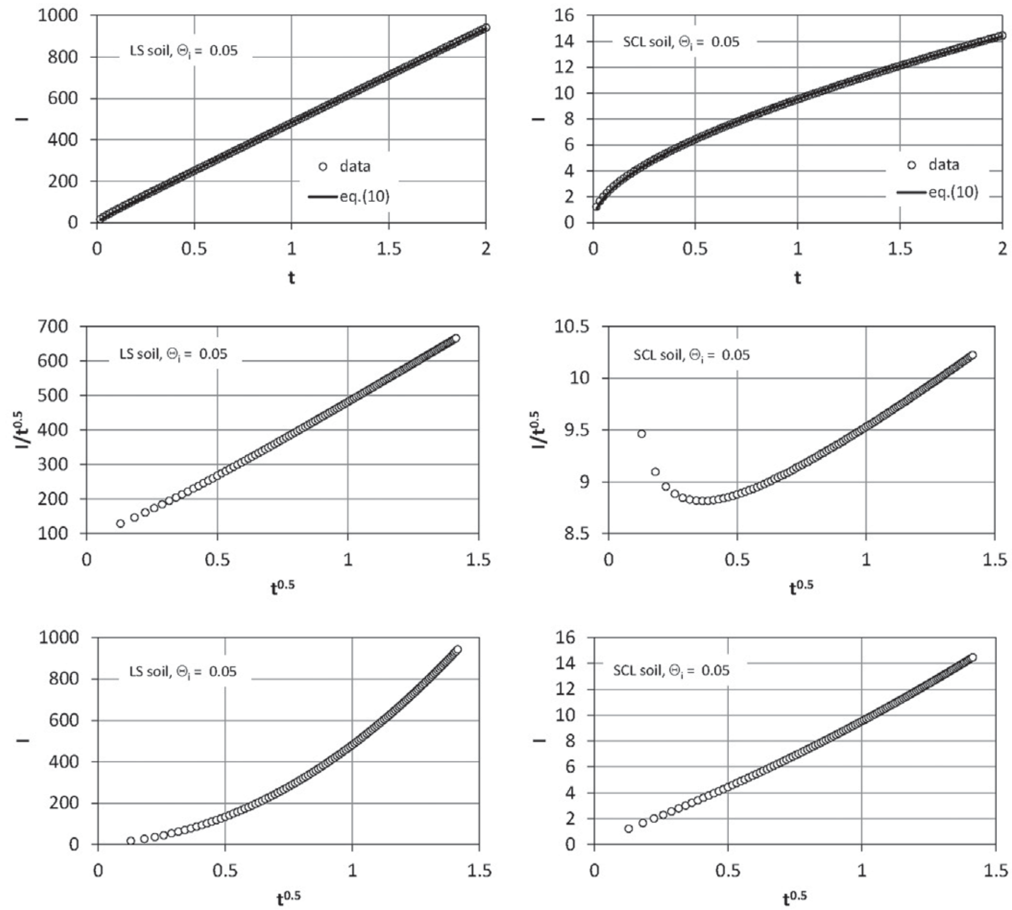

Fig. 2. Representation of the infiltration data obtained with the H50d0 scenario (depth of ponding $H = 50$ mm and ring insertion depth $d = 0$ mm) for the initially dry (initial effective saturation $\Theta_i = 0.05$) loamy sand (LS) and silty clay loam (SCL) soils on plots of cumulative infiltration, I (mm), vs. time, t (h), $I/t^{0.5}$ vs. $t^{0.5}$ (cumulative linearization method), and I vs. $t^{0.5}$.

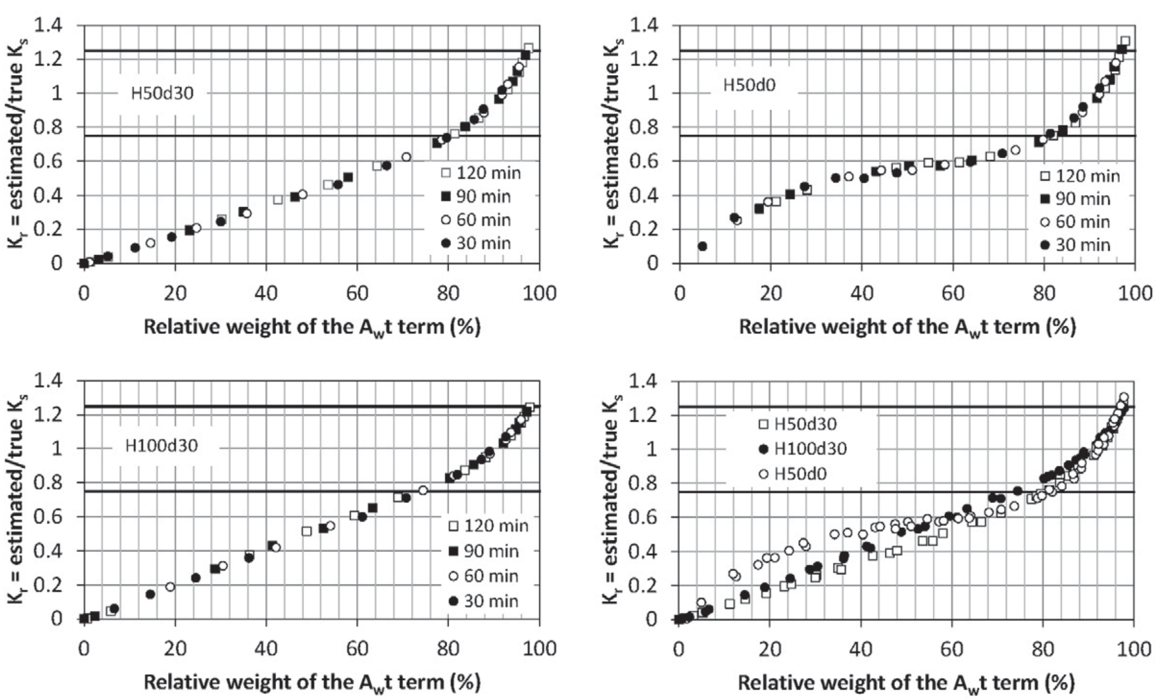

Fig. 3. Ratio K_r between the estimated and the true saturated soil hydraulic conductivity, K_s, against the weight of the $A_w \times t$ term on total infiltration for different scenarios and durations of the run. H is the ponding depth and d is the ring insertion depth,

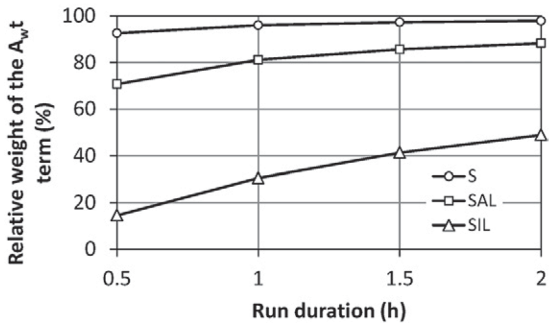

Fig. 4. Example of the relationship between the run duration and the relative weight of the $A_w \times t$ term on total infiltration for different, initially wet (initial effective saturation $\Theta_i = 0.4$), sand (S), sandy loam (SAL), and silt loam (SIL) soils and the H100d30 scenario (depth of ponding $H = 100$ mm and ring insertion depth $d = 30$ mm).

infiltration method, and inaccuracies of this latter method were attributed to a too-short infiltration time. Taking into account that steady-state infiltration follows the transient infiltration stage, it seems plausible to believe that the theory behind the approach of Reynolds and Elrick (1990) is more robust than that at the base of the Wu method. Some support for this interpretation can be found in the recent literature because, according to Stewart and Abou Najm (2018), the a constant of Eq. [12] should be set at 0.45 instead of 0.9084. However, a more specific investigation should be performed to verify the validity of the suggested explanation.

A practical way to improve the K_s calculations with the Wu method could be developing the K_r vs. run duration relationship for given soil and r, H, and Θ_i values (Table 3), and then using this relationship to estimate the range of plausible durations of the run, i.e., those yielding $0.75 \leq K_r \leq 1.25$. Testing the soundness of this procedure, and also establishing the interest to follow this route, could be done in the future.

Conclusions

Flow from a single-ring PI into initially unsaturated soil goes through an initial transient phase of decreasing rates and then approaches steady state. Applying a multilevel steady-state approach to determine K_s requires using reliable steady-state infiltration rate data for each level. However, infiltration data are commonly collected with runs that do not exceed a few hours at the most, and the available experimental information could be not enough to establish with good confidence if near steady state was reached at the end of the run or not. Equilibration time issues could be overcome by performing a single-level experiment and using a transient data analysis procedure such as the Wu method.

A first conclusion of this investigation was that, with a run duration of practical interest, the PI should be expected to yield more accurate estimates of K_s in coarse-textured soils than in fine-textured soils even if the transient method is used instead of the steady-state one.

Performing a three-level experiment and analyzing the estimated steady-state infiltration rates with both the TPD (first two levels) and MPD (all levels simultaneously) approaches is a way to predict the reliability of the estimated K_s value. Attainment of near-steady-state infiltration rates for each water level and, consequently, accurate K_s calculations are signaled by similar estimates of K_s with the two approaches. In this case, the three-level experiment is only useful to make a decision about the reliability of K_s given that the estimate of K_s was already accurate with a two-level experiment. If the estimated K_s value is substantially lower with the TPD approach than the MPD one, the expectation should be that the latter approach performed better than the former one because the gradient of steady-state flow rates with H was closer to that expected but also that steady-state conditions were not reached at the end of the infiltration runs.

The transient method does not solve the K_s inaccuracy problem in fine-textured soils because obtaining accurate K_s data requires that the portion of total infiltration varying linearly with time represents a high percentage of the total infiltration, but this percentage is small in fine-textured soils when the run does not exceed a few hours. Analyzing infiltration in real time, i.e., while performing the run, could allow establishment of the relative contribution of the two terms of the used infiltration model up to a given instant and therefore adjustment of the run duration so as to improve the accuracy of the K_s determinations, at least to a certain degree.

This investigation opens some new perspective on the use of infiltration data to make predictions about the expected reliability of K_s calculations with reference to both steady-state and transient data analysis procedures. It also suggests that it should be possible to make choices about the most appropriate run duration to obtain good quality data with the transient analysis procedure. To fully utilize the advantage of the transient method, data for longer infiltration processes should be considered for finer soils. Such measurements can conveniently be obtained by an automated system such as a pressure transducer plus a datalogger. The experimental conditions simulated in this investigation were rather wide or typical in terms of soils, initial soil water content, ring radius and insertion depth, established depths of ponding, and run duration. However, not all possible cases were considered, and working with other, experimentally plausible scenarios appears advisable to hopefully reinforce the conclusions of this investigation.

Acknowledgments

All authors contributed to outline the investigation, analyze the data, discuss the results, and write the manuscript. J. Lai performed numerical simulation of the infiltration runs. This research was partially supported by the open fund of SKHL (no. SKHL1719).

References

Alagna, V., V. Bagarello, S. Di Prima, G. Giordano, and M. Iovino. 2016. Testing infiltration run effects on the estimated water transmission properties of a sandy-loam soil. Geoderma 267:24–33. doi:10.1016/j.geoderma.2015.12.029

Angulo-Jaramillo, R., V. Bagarello, M. Iovino, and L. Lassabatére. 2016.

Infiltration measurements for soil hydraulic characterization. Springer, Cham, Switzerland. doi:10.1007/978-3-319-31788-5

Angulo-Jaramillo, R., J.-P. Vandervaere, S. Roulier, J.L. Thony, J.P. Gaudet, and M. Vauclin. 2000. Field measurement of soil surface hydraulic properties by disc and ring infiltrometers: A review and recent developments. Soil Tillage Res. 55:1–29. doi:10.1016/S0167-1987(00)00098-2

Bagarello, V., G. Baiamonte, M. Castellini, S. Di Prima, and M. Iovino. 2014. A comparison between the single ring pressure infiltrometer and simplified falling head techniques. Hydrol. Processes 28:4843–4853. doi:10.1002/hyp.9980

Bagarello, V., C. Di Stefano, M. Iovino, and A. Sgroi. 2013a. Using a transient infiltrometric technique for intensively sampling field-saturated hydraulic conductivity of a clay soil in two runoff plots. Hydrol. Processes 27:3415–3423. doi:10.1002/hyp.9448

Bagarello, V., and G. Giordano. 1999. Comparison of procedures to estimate steady flow rate in field measurement of saturated hydraulic conductivity with the Guelph permeameter method. J. Agric. Eng. Res. 74:63–71. doi:10.1006/jaer.1999.0437

Bagarello, V., and M. Iovino. 1999. Spatial and temporal variability of saturated hydraulic conductivity in a central Sicily soil. In: J. Feyen and K. Wiyo, editors, Proceedings of the International Workshop of EurAgEng's Field of Interest on Soil and Water: Modelling of Transport Processes in Soils, Leuven, Belgium. 24–26 Nov. 1999. Wageningen Pers, Wageningen, the Netherlands. p. 249–256.

Bagarello, V., M. Iovino, and J. Lai. 2013b. Field and numerical tests of the two-ponding depth procedure for analysis of single-ring pressure infiltrometer data. Pedosphere 23:779–789. doi:10.1016/S1002-0160(13)60069-7

Bagarello, V., M. Iovino, and J. Lai. 2016. Testing steady-state analysis of single-ring and square pressure infiltrometer data. Geoderma 261:101–109. doi:10.1016/j.geoderma.2015.07.002

Bagarello, V., M. Iovino, and W.D. Reynolds. 1999. Measuring hydraulic conductivity in a cracking clay soil using the Guelph permeameter. Trans. ASAE 42:957–964. doi:10.13031/2013.13276

Bagarello, V., M. Iovino, and G. Tusa. 2000. Factors affecting measurement of the near-saturated soil hydraulic conductivity. Soil Sci. Soc. Am. J. 64:1203–1210. doi:10.2136/sssaj2000.6441203x

Bagarello, V., S. Sferlazza, and A. Sgroi. 2009. Comparing two methods of analysis of single-ring infiltrometer data for a sandy-loam soil. Geoderma 149:415–420. doi:10.1016/j.geoderma.2008.12.022

Bagarello, V., and A. Sgroi. 2004. Using the single-ring infiltrometer method to detect temporal changes in surface soil field-saturated hydraulic conductivity. Soil Tillage Res. 76:13–24. doi:10.1016/j.still.2003.08.008

Bautista, E., A.W. Warrick, J.L. Schlegel, K.R. Thorp, and D.J. Hunsaker. 2016. Approximate furrow infiltration model for time-variable ponding depth. J. Irrig. Drain. Eng. 142(11). doi:10.1061/(ASCE)IR.1943-4774.0001057

Bouma, J. 1982. Measuring the hydraulic conductivity of soil horizons with continuous macropores. Soil Sci. Soc. Am. J. 46:438–441. doi:10.2136/sssaj1982.03615995004600020047x

Carsel, R.F., and R.S. Parrish. 1988. Developing joint probability distributions of soil water retention characteristics. Water Resour. Res. 24:755–769. doi:10.1029/WR024i005p00755

Celia, M.A., E.T. Boulouton, and R.L. Zarba. 1990. A general mass conservation numerical solution for the unsaturated flow equation. Water Resour. Res. 26:1483–1496. doi:10.1029/WR026i007p01483

Chen, L.-J., Q. Feng, F.-R. Li, and C.S. Li. 2015. Simulation of soil water and salt transfer under mulched furrow irrigation with saline water. Geoderma 241–242:87–96. doi:10.1016/j.geoderma.2014.11.007

Ciollaro, G., and N. Lamaddalena. 1998. Effect of tillage on the hydraulic properties of a vertic soil. J. Agric. Eng. Res. 71:147–155. doi:10.1006/jaer.1998.0312

Cook, F.J., and A. Broeren. 1994. Six methods for determining sorptivity and hydraulic conductivity with disc permeameters. Soil Sci. 157:2–11. doi:10.1097/00010694-199401000-00002

Di Prima, S., L. Lassabatere, J. Rodrigo-Comino, R. Marrosu, M. Pulido, R. Angulo-Jaramillo, et al.. 2018. Comparing transient and steady-state analysis of single-ring infiltrometer data for an abandoned field affected by fire in eastern Spain. Water 10:514. doi:10.3390/w10040514

Dohnal, M., T. Vogel, J. Dusek, J. Votrubova, and M. Tesar. 2016. Interpretation of ponded infiltration data using numerical experiments. J. Hydrol. Hydromech. 64:289–299. doi:10.1515/johh-2016-0020

Dušek, J., M. Dohnal, and T. Vogel. 2009. Numerical analysis of ponded infiltration experiment under different experimental conditions. Soil Water Res. 4:S22–S27. doi:10.17221/1368-SWR

Elrick, D.E., and W.D. Reynolds. 1992a. Methods for analyzing constant-head well permeameter da-ta. Soil Sci. Soc. Am. J. 56:320–323. doi:10.2136/sssaj1992.03615995005600010052x

Elrick, D.E., and W.D. Reynolds. 1992b. Infiltration from constant-head well permeameters and infiltrometers. In: G.C. Topp et al., editors, Advances in measurement of soil physical properties: Bringing theory into practice. SSSA Spec. Publ. 30. SSSA, Madison, WI. p. 1–24. doi:10.2136/sssaspecpub30.c1

Gardner, W.R. 1958. Some steady state solutions of the unsaturated moisture flow equation with application to evaporation from a water table. Soil Sci. 85:228–232. doi:10.1097/00010694-195804000-00006

Gómez, J.A., K. Vanderlinden, and M.A. Nearing. 2005. Spatial variability of surface roughness and hydraulic conductivity after disk tillage: Implications for runoff variability. J. Hydrol. 311:143–156. doi:10.1016/j.jhydrol.2005.01.014

Haverkamp, R., M. Vauclin, J. Touma, P.J. Wierenga, and G. Vachaud. 1977. A comparison of numerical simulation models for one-dimensional infiltration. Soil Sci. Soc. Am. J. 41:285–294. doi:10.2136/sssaj1977.03615995004100020024x

Hinnell, A.C., N. Lazarovitch, and A.W. Warrick. 2009. Explicit infiltration function for boreholes under constant head conditions. Water Resour. Res. 45:W10429.

Jacques, D., J. Šimůnek, D. Mallants, and M.Th. van Genuchten. 2006. Operator-splitting errors in coupled reactive transport codes for transient variably saturated flow and contaminant transport in layered soil profiles. J. Contam. Hydrol. 88:197–218. doi:10.1016/j.jconhyd.2006.06.008

Lai, J., Y. Luo, and L. Ren. 2010. Buffer index effects on hydraulic conductivity measurements using numerical simulations of double-ring infiltration. Soil Sci. Soc. Am. J. 74:1526–1536. doi:10.2136/sssaj2009.0450

Lai, J., and L. Ren. 2007. Assessing the size dependency of measured hydraulic conductivity using double-ring infiltrometers and numerical simulation. Soil Sci. Soc. Am. J. 71:1667–1675. doi:10.2136/sssaj2006.0227

Lassabatère, L., R. Angulo-Jaramillo, J.M. Soria Ugalde, R. Cuenca, I. Braud, and R. Haverkamp. 2006. Beerkan estimation of soil transfer parameters through infiltration experiments: BEST. Soil Sci. Soc. Am. J. 70:521–532. doi:10.2136/sssaj2005.0026

Mallants, D., B.P. Mohanty, A. Vervoort, and J. Feyen. 1997. Spatial analysis of saturated hydraulic conductivity in a soil with macropores. Soil Technol. 10:115–131. doi:10.1016/S0933-3630(96)00093-1

Mertens, J., D. Jacques, J. Vanderborght, and J. Feyen. 2002. Characterisation of the field-saturated hydraulic conductivity on a hillslope: In situ single ring pressure infiltrometer measurements. J. Hydrol. 263:217–229. doi:10.1016/S0022-1694(02)00052-5

Mualem, Y. 1976. A new model for predicting the hydraulic conductivity of unsaturated porous media. Water Resour. Res. 12:513–522. doi:10.1029/WR012i003p00513

Papanicolaou, A.N., M. Elhakeem, C.G. Wilson, C.L. Burras, L.T. West, H. Lin, et al. 2015. Spatial variability of saturated hydraulic conductivity at the hillslope scale: Understanding the role of land management and erosional effect. Geoderma 243–244:58–68. doi:10.1016/j.geoderma.2014.12.010

Rathfelder, K., and L.M. Abriola. 1994. Mass conservative numerical solutions of the head-based Richards equation. Water Resour. Res. 30:2579–2586. doi:10.1029/94WR01302

Reynolds, W.D. 2008. Saturated hydraulic properties: Ring infiltrometer In: M.R. Carter and E.G. Gregorich, editors, Soil sampling and methods of analysis. 2nd ed. CRC Press, Boca Raton, FL. p. 1043–1056.

Reynolds, W.D. 2010. Measuring soil hydraulic properties using a cased borehole permeameter: Steady flow analyses. Vadose Zone J. 9:637–652. doi:10.2136/vzj2009.0136

Reynolds, W.D. 2011. Measuring soil hydraulic properties using a cased borehole permeameter: Falling-head analysis. Vadose Zone J. 10:999–1015. doi:10.2136/vzj2010.0145

Reynolds, W.D. 2013. An assessment of borehole infiltration analyses for measuring field-saturated hydraulic conductivity in the vadose zone. Eng. Geol. 159:119–130. doi:10.1016/j.enggeo.2013.02.006

Reynolds, W.D., B.T. Bowman, R.R. Brunke, C.F. Drury, and C.S. Tan. 2000. Comparison of tension infiltrometer, pressure infiltrometer, and soil core estimates of saturated hydraulic conductivity. Soil Sci. Soc. Am. J. 64:478–484. doi:10.2136/sssaj2000.642478x

Reynolds, W.D., and D.E. Elrick. 1985. In situ measurement of field-saturated hydraulic conductivity, sorptivity and the a-parameter using the Guelph permeameter. Soil Sci. 140:292–302. doi:10.1097/00010694-198510000-00008

Reynolds, W.D., and D.E. Elrick. 1987. A laboratory and numerical assessment of the Guelph permeameter method. Soil Sci. 144:282–299. doi:10.1097/00010694-198710000-00008

Reynolds, W.D., and D.E. Elrick. 1990. Ponded infiltration from a single ring: I. Analysis of steady flow. Soil Sci. Soc. Am. J. 54:1233–1241. doi:10.2136/sssaj1990.03615995005400050006x

Reynolds, W.D., and D.E. Elrick. 1991. Determination of hydraulic conductivity using a tension infiltrometer. Soil Sci. Soc. Am. J. 55:633–639. doi:10.2136/sssaj1991.03615995005500030001x

Reynolds, W.D., and D.E. Elrick. 2002. Pressure infiltrometer In: J.H. Dane and G.C. Topp, editors, Methods of soil analysis. Part 4. Physical methods. SSSA Book Ser. 5. SSSA, Madison, WI. p. 826–836. doi:10.2136/sssabookser5.4.c32

Reynolds, W.D., D.E. Elrick, and B.E. Clothier. 1985. The constant head well permeameter: Effect of unsaturated flow. Soil Sci. 139:172–180. doi:10.1097/00010694-198502000-00011

Reynolds, W.D., D.E. Elrick, and E.G. Youngs. 2002a. Ring or cylinder infiltrometers (vadose zone). In: J.H. Dane and G.C. Topp, editors, Methods of soil analysis. Part 4. Physical methods. SSSA Book Ser. 5. SSSA, Madison, WI. p. 818–820. doi:10.2136/sssabookser5.4.c32

Reynolds, W.D., D.E. Elrick, and E.G. Youngs. 2002b. Single-ring and double- or concentric-ring infiltrometers. In: J.H. Dane and G.C. Topp, editors, Methods of soil analysis. Part 4. Physical methods. SSSA Book Ser. 5. SSSA, Madison, WI. p. 821–826. doi:10.2136/sssabookser5.4.c32

Reynolds, W.D., S.R. Vieira, and G.C. Topp. 1992. An assessment of the single-head analysis for the constant head well permeameter. Can. J. Soil Sci. 72:489–501. doi:10.4141/cjss92-041

Reynolds, W.D., and W.D. Zebchuk. 1996. Hydraulic conductivity in a clay soil: Two measurement techniques and spatial characterization. Soil Sci. Soc. Am. J. 60:1679–1685. doi:10.2136/sssaj1996.03615995006000060011x

Rezaei, M., P. Seuntjens, R. Shahidi, I. Joris, W. Boenne, B. Al-Barri, and W. Cornelis. 2016. The relevance of in-situ and laboratory characterization of sandy soil hydraulic properties for soil water simulations. J. Hydrol. 534:251–265. doi:10.1016/j.jhydrol.2015.12.062

Shan, Y., and Q. Wang. 2012. Simulation of salinity distribution in the overlap zone with double-point-source drip irrigation using HYDRUS-3D. Aust. J. Crop Sci. 6:238–247.

Šimůnek, J., M. Šejan, and M.Th. van Genuchten. 2007. The HYDRUS software package for simulating two- and three-dimensional movement of water, heat, and multiple solutes in variably-saturated media. Tech. Manual, Version 1.0. PC Progress, Prague, Czech Republic.

Smettem, K.R.J., P.J. Ross, R. Haverkamp, and J.-Y. Parlange. 1995. Three-dimensional analysis of infiltration from the disk infiltrometer: 3. Parameter estimation using a double-disk tension infiltrometer. Water Resour. Res. 31:2491–2495. doi:10.1029/95WR01722

Smiles, D.E., and J.H. Knight. 1976. A note on the use of the Philip infiltration equation. Aust. J. Soil Res. 14:103–108. doi:10.1071/SR9760103

Stewart, R.D., and M.R. Abou Najm. 2018. A comprehensive model for single ring infiltration: I. Initial water content and soil hydraulic properties. Soil Sci. Soc. Am. J. 82:548–557. doi:10.2136/sssaj2017.09.0313

Vandervaere, J.P., M. Vauclin, and D.E. Elrick. 2000. Transient flow from tension infiltrometers: I. The two-parameter equation. Soil Sci. Soc. Am. J. 64:1263–1272. doi:10.2136/sssaj2000.6441263x

van Genuchten, M.Th. 1980. A closed-form equation for predicting the hydraulic conductivity of unsaturated soils. Soil Sci. Soc. Am. J. 44:892–898. doi:10.2136/sssaj1980.03615995004400050002x

Vauclin, M., D.E. Elrick, J.L. Thony, G. Vachaud, Ph. Revol, and P. Ruelle. 1994. Hydraulic conductivity measurements of the spatial variability of a loamy soil. Soil Technol. 7:181–195. doi:10.1016/0933-3630(94)90020-5

Verbist, K., J. Baetens, W.M. Cornelis, D. Gabriels, C. Torres, and G. Soto. 2009. Hydraulic conductivity as influenced by stoniness in degraded drylands of Chile. Soil Sci. Soc. Am. J. 73:471–484. doi:10.2136/sssaj2008.0066

Verbist, K.M.J., W.M. Cornelis, S. Torfs, and D. Gabriels. 2013. Comparing methods to determine hydraulic conductivities on stony soils. Soil Sci. Soc. Am. J. 77:25–42. doi:10.2136/sssaj2012.0025

Verbist, K., S. Torfs, W.M. Cornelis, R. Oyarzún, G. Soto, and D. Gabriels. 2010. Comparison of single- and double-ring infiltrometer methods on stony soils. Vadose Zone J. 9:462–475. doi:10.2136/vzj2009.0058

Wu, L., and L. Pan. 1997. A generalized solution to infiltration from single-ring infiltrometers by scaling. Soil Sci. Soc. Am. J. 61:1318–1322. doi:10.2136/sssaj1997.03615995006100050005x

Wu, L., L. Pan, J. Mitchell, and B. Sanden. 1999. Measuring saturated hydraulic conductivity using a generalized solution for single-ring infiltrometers. Soil Sci. Soc. Am. J. 63:788–792. doi:10.2136/sssaj1999.634788x

Wu, L., J.B. Swan, J.L. Nieber, and R.R. Allmaras. 1993. Soil-macropore and layer influences on saturated hydraulic conductivity measured with borehole permeameters. Soil Sci. Soc. Am. J. 57:917–923. doi:10.2136/sssaj1993.03615995005700040006x